Cell, Vol. 98, 69–80, July 9, 1999, Copyright ©1999 by Cell Press

Endomembrane Trafficking of Ras: The CAAX Motif Targets Proteins to the ER and Golgi

Edwin Choy, Vi K. Chiu, Joseph Silletti, Marianna Feoktistov, Takashi Morimoto, David Michaelson, Ivan E. Ivanov, and Mark R. Philips*
Departments of Medicine and Cell Biology
New York University School of Medicine
New York, New York 10016

Summary

We show that Nras is transiently localized in the Golgi prior to the plasma membrane (PM). Moreover, green fluorescent protein (GFP)-tagged Nras illuminated motile, peri-Golgi vesicles, and prolonged BFA treatment blocked PM expression. GFP-Hras colocalized with GFP-Nras, but GFP-Kras4B revealed less Golgi and no vesicular fluorescence. Whereas a secondary membrane targeting signal was required for PM expression, the CAAX motif alone was necessary and sufficient to target proteins to the endomembrane where they were methylated, a modification required for efficient membrane association. Thus, prenylated CAAX proteins do not associate directly with the PM but instead associate with the endomembrane and are subsequently transported to the PM, a process that requires a secondary targeting motif.

Introduction

Ras GTPases are among a class of proteins that are targeted from the cytosol to the inner leaflet of the plasma membrane (PM) by posttranslational modification of a C-terminal CAAX motif (Clarke, 1992). The CAAX motif is necessary and sufficient for recognition by the first in a series of enzymes that sequentially modify the C terminus of CAAX proteins (Reiss et al., 1990). This first modification, prenylation, is catalyzed by one of two soluble prenyltransferases that attach, respectively, a farnesyl or geranylgeranyl lipid via a stable thioether linkage to the CAAX cysteine. The substrate specificity for farnesyltransferase versus geranylgeranyltransferase is determined by the residue in the X position of the CAAX motif (Casey and Seabra, 1996). Next, the prenyl-CAAX motif is recognized by a specific protease that cleaves the AAX residues, leaving the prenylcysteine as the new C terminus. The modified cysteine is then recognized by a prenylcysteine carboxyl methyltransferase (pcCMT) that methylesterifies the α carboxyl group. In the case of Nras and Hras, but not Kras, a further modification is made in the hypervariable region of the protein just upstream of the CAAX motif whereby one or two other cysteine residues are modified by palmitic acid via a labile thioester linkage (Hancock et al., 1989). The net result of these sequential modifications is to generate a hydrophobic C-terminal domain on an otherwise hydrophilic molecule. In the case of Kras, a polybasic sequence in the hypervariable domain upstream of the CAAX motif substitutes for palmitoylated cysteines in acting as a second required PM targeting signal (Hancock et al., 1990). Whether the modified C terminus of processed ras mediates protein–phospholipid or protein–protein interactions or both is unknown.

Whereas the prenyltransferases are soluble (Casey and Seabra, 1996), the activities of the enzymes that act subsequent to prenyltransferase, including the prenyl-CAAX protease (Hancock et al., 1991a), pcCMT (Pillinger et al., 1994), and protein palmitoyltransferase (Kasinathan et al., 1990), are associated with membranes. Two of these three classes of enzymes, the prenyl-CAAX protease and pcCMT, were recently characterized at the molecular level, allowing unambiguous subcellular localization. Genetic screens of *Saccharomyces cerevisiae* identified genes for two metalloproteases with farnesyl-CAAX protease activity, *STE24/AFC1* (Boyartchuk et al., 1997; Fujimura-Kamada et al., 1997) and *RCE1* (Boyartchuk et al., 1997). Each gene predicted a polytopic membrane protein localized in the endoplasmic reticulum (ER) (Schmidt et al., 1998). Similarly, both the *S. cerevisiae* prenylcysteine carboxyl methyltransferase Ste14p (Romano et al., 1998) and its human homolog pcCMT (Dai et al., 1998) are putative polytopic membrane proteins localized in the ER. Using enhanced green fluorescent protein (GFP)-tagged pcCMT, we have demonstrated complete exclusion of pcCMT from the PM (Dai et al., 1998).

The observation that the enzymes that further modify prenylated CAAX proteins are localized in the endomembrane system has led to the hypothesis that, contrary to previous assumptions, ras is not targeted directly from the cytosol to the PM but rather takes an indirect route via the cytoplasmic face of the endomembrane system. To test this hypothesis, we expressed a library of CAAX proteins tagged with GFP and determined their localization in living cells using high-resolution digital epifluorescence microscopy. Ras was expressed in the Golgi and peri-Golgi vesicles prior to PM expression. Moreover, our results indicate that the CAAX motif alone targets proteins to the endomembrane system where they are methylated and that further trafficking to the PM is dependent on either palmitoylation or a polybasic motif. Thus, rather than promoting nonspecific membrane association, prenylation mediates specific association with the ER and Golgi membranes, and further processing allows engagement of a transport pathway to the PM.

Results

Ras Is Expressed in the Golgi

To test the hypothesis that ras molecules encounter prenyl-CAAX-modifying enzymes in the endomembrane system, we tagged the N terminus of Nras with GFP, expressed the fusion protein in a variety of cultured cells

*To whom correspondence should be addressed (e-mail: philim01@med.nyu.edu).

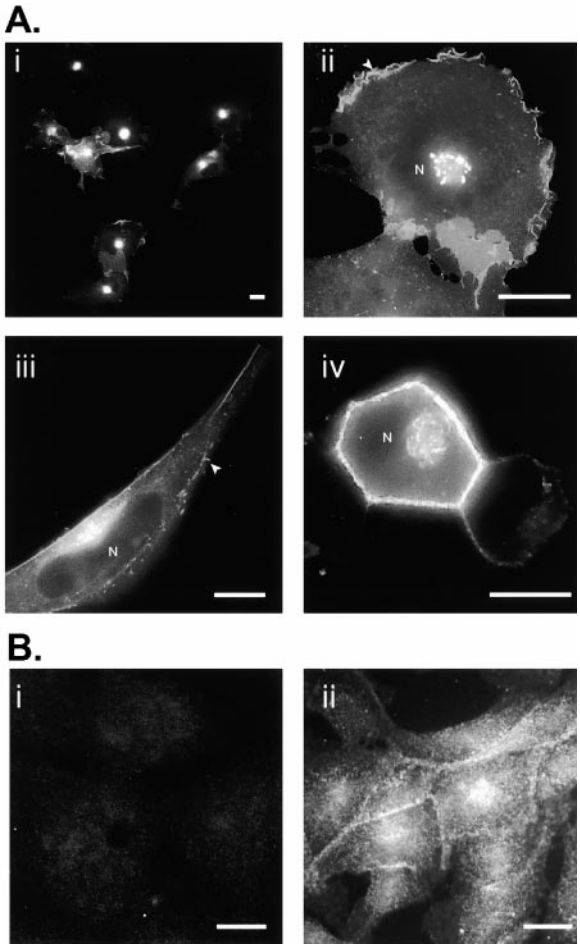

Figure 1. Subcellular Localization of GFP-Nras and Endogenous Ras

(A) COS-1 (i and ii), CHO (iii), and MDCK (iv) cells were transfected with GFP-Nras and examined alive by epifluorescence microscopy. Arrowheads (ii and iii) indicate lamellipodia.

(B) Fixed MDCK cells stained with TRITC-conjugated anti-CD20 control antibody (i) or TRITC-conjugated Y13-258 anti-ras antibody. Bars = 10 μm.

by transfection, and observed its subcellular localization in living cells by epifluorescence microscopy. Although, as expected, GFP-Nras was expressed in the PM (Figure 1), the most prominent feature in COS-1 cells was an intense, compact (~2 μm), and well-delineated area of fluorescence adjacent to the nucleus (Figure $1A_i$). In some cells, a multivesicular morphology of this structure, suggestive of the Golgi apparatus, could be resolved (Figure $1A_{ii}$). This feature was not limited to COS-1 cells but was also observed in CHO (Figure $1A_{iii}$) and MDCK cells (Figure $1A_{iv}$), as well as in murine fibroblasts and human bladder carcinoma cells (not shown). The most prominent PM fluorescence in both COS-1 and CHO cells was apparent in lamellipodia (arrowheads, Figures $1A_{ii}$ and $1A_{iii}$) that were primarily peripheral in COS-1 cells but both peripheral and dorsal in CHO cells. GFP-Nras was observed both in the basolateral membrane of polarized MDCK cells (Figure $1A_{iv}$) and in the apical membrane, primarily in lamellipodia (not shown).

To exclude the possibility that the perinuclear fluorescence of GFP-ras-transfected cells was due to mislocalization caused either by the GFP epitope or overexpression, we examined the localization of endogenous ras by direct immunofluorescence. Although the resolution afforded by immunofluorescence in fixed, permeabilized MDCK cells was markedly inferior to that achieved in live GFP-Nras-transfected cells, endogenous ras was clearly observed in both PM and the perinuclear region (Figure 1B). Similar results were obtained with COS-1 cells.

To determine if the perinuclear fluorescence was due to ras in the Golgi apparatus, we colocalized by confocal microscopy GFP-Nras and Golgi markers. CHO cells transfected with GFP-Nras and fixed, permeabilized, and stained for mannosidase II revealed colocalization in the perinuclear region (Figure $2A_i$). Similarly, COS-1 cells transfected with GFP-Nras, treated with a Golgi-specific vital stain (Texas red–conjugated BODIPY ceramide C_6), and observed alive revealed colocalization (Figure $2A_{ii}$). To exclude the possibility that the apparent colocalization was due to PM-derived ras trafficking through the endosomal recycling compartment that is closely associated with the Golgi, we tested for sensitivity to brefeldin A (BFA), an agent known to cause dispersal of the *cis* and medial Golgi (Lippincott-Schwartz et al., 1989). BFA induced dispersal of the intensely fluorescent perinuclear structure illuminated by GFP-Nras (Figure 2B). To confirm Golgi localization of GFP-Nras, we examined by electron microscopy thin frozen sections of GFP-Nras-transfected COS-1 cells that were labeled with an anti-GFP antiserum and colloidal gold-conjugated protein A (Figure 2C). As expected, gold particles decorated the PM of transfected cells. In addition, the label was found throughout the Golgi stack. To confirm Golgi localization of ras in untransfected cells, we examined the distribution of endogenous ras by subcellular fractionation of [^{35}S]methionine/cysteine-labeled MDCK cells. Ras was present in each membrane fraction (Table 1), and the specific activity observed in the Golgi-enriched fraction was 3-fold that observed in the PM-enriched fraction. Thus, both GFP-Nras and endogenous ras are expressed in the Golgi.

Trafficking of Nras

To test the hypothesis that GFP-Nras is targeted to the PM via the Golgi, we determined the relative kinetics of GFP-Nras expression in the two membrane compartments. After transient transfection, Golgi fluorescence, in the absence of PM fluorescence, was readily apparent by 5 to 8 hr (Figure $3A_i$). In contrast, 12–18 hr of culture posttransfection was required to visualize both Golgi and PM (Figure $3A_{ii}$). When cells were allowed to express GFP-Nras for 16 hr and then treated with cycloheximide for 6 hr to block protein synthesis, the intensity of Golgi fluorescence markedly diminished, whereas that of the PM was maintained (Figure $3A_{iii}$), consistent with a chase of GFP-Nras from the Golgi to the PM.

To more effectively synchronize GFP-Nras expression, we constructed a plasmid in which GFP-Nras was placed under the control of an IPTG-inducible promotor and stably transfected CHO cells that constitutively express Lac repressor. Repression of GFP-Nras expression in the absence of IPTG was efficient in each of

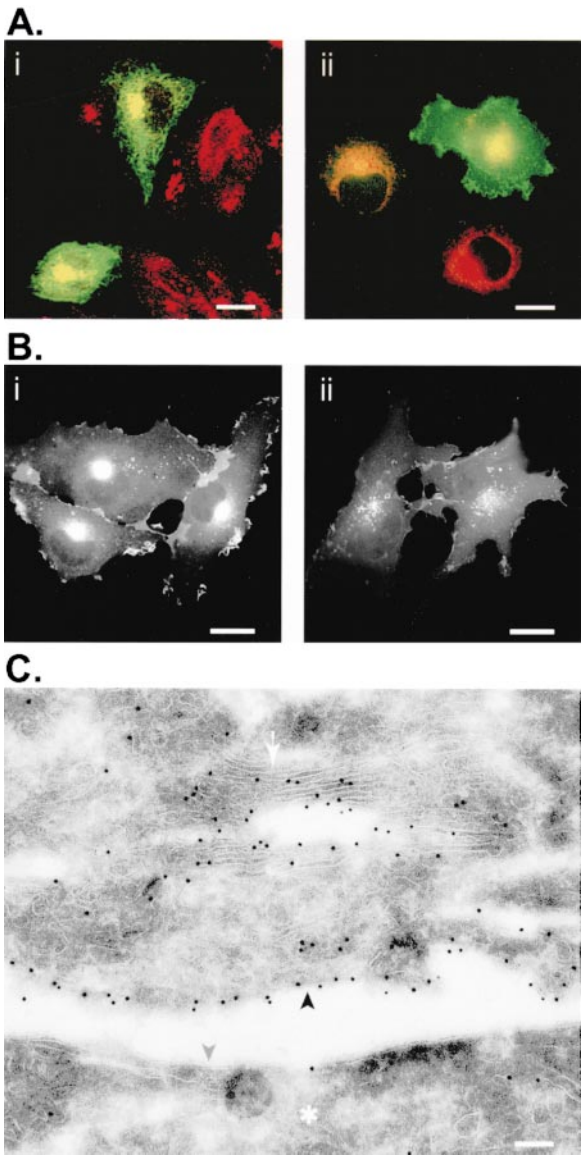

Figure 2. GFP-Nras Is Expressed in the Golgi Apparatus

(A) CHO cells transfected with GFP-Nras were fixed and stained for the Golgi marker mannosidase II (Texas red) and analyzed by confocal microscopy (i). COS-1 cells transfected with GFP-Nras and stained with a Golgi-specific vital dye (TR-BODIPY ceramide C_6) and examined alive (ii). Yellow pseudocolor indicates colocalization. Bars = 10 μm.

(B) COS-1 cells expressing GFP-Nras for 24 hr were treated for 30 min with medium alone (i) or 5 μg/ml BFA (ii) and examined alive. Bars = 10 μm.

(C) Frozen ultrathin sections of COS-1 cells transfected with GFP-Nras were treated with anti-GFP antiserum followed by protein A–gold 10 nm conjugates and examined with an electron microscopy. The asterisk indicates an untransfected adjacent cell. Arrowheads indicate the PM (black, transfected; gray, untransfected). Arrow indicates Golgi stacks. Bar = 100 nm.

the three cell lines established, as was induction in the presence of IPTG (Figure 3B). Whereas Golgi fluorescence was observed as early as 8 hr after induction (Figure $3B_i$), PM fluorescence was evident only after 16 hr of IPTG induction (Figure $3B_{ii}$). Cycloheximide had an effect on IPTG-induced GFP-Nras similar to that observed on the transiently expressed molecule ($3B_{iii}$). Thus, Golgi expression of GFP-Nras preceded PM expression and could be chased into the PM. This suggests that if Golgi and PM expression of GFP-Nras are related by vectorial vesicular transport, the transport is anterograde relative to the secretory pathway.

To compare the fluorescence pattern of GFP-Nras to that of GFP-tagged examples of a transmembrane protein that transits the secretory pathway and that of a posttranslationally modified protein that is targeted rapidly and directly to the PM, we transfected cells with VSVG-GFP (Presley et al., 1997) and Fyn-GFP (van't Hof and Resh, 1997), respectively. We utilized a temperature-sensitive mutant of VSVG-GFP that illuminates the ER at the nonpermissive temperature (Presley et al., 1997). However, like GFP-Nras, at the permissive temperature VSVG-GFP revealed PM and intense Golgi fluorescence without ER (Figure $3C_i$), suggesting that at steady state the flux and local concentrations of VSVG are such that GFP preferentially reports Golgi localization. In contrast, Fyn-GFP was apparent only in the PM (Figure $3C_{ii}$). Each of these fluorescence patterns was distinct from that of the cytosolic pattern revealed by transfecting the same cells with GFP-NrasC186S, a mutant that cannot be posttranslationally processed because the CAAX cysteine is changed to serine (Figure $3C_{iii}$).

VSVG-GFP has been observed in rapidly motile, relatively large (0.1–1.5 μm) tubulovesicular peri-Golgi vesicles in living COS-1 cells after transient transfection (Presley et al., 1997). We observed GFP-Nras in strikingly similar structures in living COS-1 cells (Figure 3D). Like VSVG-GFP-illuminated vesicles, we observed both rapidly motile (0.1–1 μm/s) vesicles (arrows) and coalescence of vesicles into tubular structures (arrowhead). Also like VSVG-GFP, the GFP-Nras-illuminated vesicles moved in a saltatory fashion along linear tracks, suggestive of microtubules. Thus, the transmembrane protein VSVG-GFP that is transported by the secretory pathway and GFP-Nras appear to be expressed in similar vesicular structures. To test whether vesicular transport is required for PM expression of GFP-Nras, we treated cells transfected with GFP-Nras or Fyn-GFP with BFA for 10 hr, beginning 3 hr after transfection when the cells had recovered but no fluorescence was apparent. Whereas prolonged BFA treatment had no effect on Fyn-GFP expression in the PM (Figure $3E_{iii}$), GFP-Nras expression in this compartment was blocked (Figures $3E_i$ and $3E_{ii}$). Thus, vesicular transport is required for PM expression of GFP-Nras.

To test further the hypothesis that ras transits components of the secretory pathway, we performed pulse–chase analyses of ras in subcellular fractions. We chose MDCK cells for these studies because of the well-established methods for isolating Golgi from other membranes (Table 1). However, using conventional methods, we were unable to separate PM from smooth microsomes: the smooth membrane fraction contained both Na/K ATPase and pcCMT activities (not shown). To facilitate detection of Nras, we produced lines of MDCK cells that stably express GFP-Nras and followed the pulse-labeled fusion protein in subcellular fractions by immunoprecipitating with an antibody to GFP (Figure 4A).

Table 1. Subcellular Distribution of Ras in MDCK Cells

Fraction	Protein (mg)	Na/K ATPase (μmol/mg/hr)	Galactosyl Transferase (μmol/mg/hr)	RNA (mg)	Ras[a]
Cytosol	**23.7**	0.006	0.0005	2.01	1.15 ± 0.40
PM+SER	0.88	**3.207**	0.1495	0.07	1.00
Golgi	0.21	1.154	**1.0470**	0.01	**2.98 ± 0.80**
RER	5.23	0.318	0.0412	**3.44**	0.40 ± 0.11

Confluent MDCK cells were homogenized and fractionated as described in the Experimental Procedures. Total protein and RNA content of each fraction from a representative experiment is given, as are the specific activities of PM and Golgi marker enzymes (Na/K ATPase and galactosyl transferase, respectively). The same cells grown in parallel were metabolically labeled with [^{35}S]methionine/cysteine for 30 min, chased with cold methionine/cysteine for 60 min, and then subjected to identical fractionation. Ras was immunoprecipitated from detergent extracts of each fraction and quantitated by SDS-PAGE and phosphorimager. The bold result in each column indicates the peak value.
[a] The values given for Ras represent specific activities relative to that of the plasma membrane fraction and are given as mean ± SEM, n = 4.

Immediately following the pulse, 95% of nascent GFP-Nras was located in the cytosol, and this pool decayed slowly with a half-life of 2 hr. Metabolic labeling with [^{3}H]mevalonate revealed that the soluble pool was prenylated (not shown), suggesting that whereas farnesylation may be efficient and immediately posttranslational, membrane association is not. To exclude the possibility that the large cytosolic pool was the result of overexpression or mislocalization of GFP-Nras, we performed a similar pulse–chase analysis on endogenous ras in MDCK cells and obtained very similar results (Figure 4B). The half-life of the cytosolic pool of endogenous ras was also 2 hr. Moreover, no more than 10% of the endogenous ras lost from the cytosol during the chase ever appeared in the membrane fractions, suggesting that membrane targeting is surprisingly inefficient and that the majority of the cytosolic pool is degraded without membrane association. Although a direct comparison of the localization of nascent ras detected by immunoprecipitation and GFP-Nras detected by fluorescence 16–48 hr after transfection may be misleading, the marked differences in the relative amounts of cytosolic ras detected suggest that GFP reports membrane-associated ras much more efficiently than soluble protein.

Immediately following the pulse, GFP-Nras was associated with both the rough and smooth microsomes, consistent with the subcellular localization of prenyl-CAAX processing enzymes, but relatively little was observed in the Golgi fraction. Subsequently, GFP-Nras was transiently observed in the Golgi-enriched fraction with a peak after 1 hr. Expression of GFP-Nras in the fraction enriched for both PM and smooth microsomes was constant over the chase period, consistent with both early and late delivery of protein to this mixed fraction. The pattern of expression of endogenous ras in the Golgi and mixed PM/smooth microsomal fractions was identical to that of GFP-Nras. When analyzed for percent of total recovered endogenous ras associated with each membrane fraction (Figure 4C), a clear pattern emerged in which maximal association of ras with the Golgi preceded maximal association with the PM-enriched fraction, concordant with our fluorescent observations. The persistence of a large pool of cytosolic ras accessible to membrane compartments and the inability to separate PM from smooth microsomes confounded efforts to establish clear precursor–product relationships between ras in the various fractions. Nevertheless, the transient expression of ras in the Golgi fraction and the sustained expression in the PM-enriched fraction but not the rough microsomes is strongly suggestive of vesicular transport.

Differential Localization of Ras Proteins

One of the two membrane localization sequences of Kras4B differs from that of Nras and Hras (Hancock et al., 1990). To determine the subcellular distribution of the three ras gene products, we tagged each with GFP (Figures 5A and 5B). In COS-1 cells (Figure 5A), GFP-Hras gave a pattern of fluorescence similar to that of GFP-Nras: PM expression, particularly in peripheral lamellipodia, and an intense, predominant Golgi fluorescence associated with peri-Golgi vesicles. In contrast, GFP-Kras4B was expressed predominantly at the PM in both peripheral and dorsal ruffles. The difference was more evident in MDCK cells (Figure 5B) that appeared to express GFP-Kras4B exclusively in the PM. However, the majority of COS-1 cells that expressed GFP-Kras4B revealed some degree of perinuclear fluorescence. Although in some cells this pattern closely resembled that observed in cells expressing GFP-Nras and GFP-Hras, the majority of GFP-Kras4B-expressing cells revealed a much less prominent and more diffuse fluorescence in the region of the Golgi. Moreover, the peri-Golgi vesicles observed with GFP-tagged Nras and Hras were not observed with GFP-Kras4B. Pulse–chase analysis of GFP-Kras4B in fractions derived from stably transfected MDCK cells revealed that the half-life of cytosolic GFP-Kras4B was one-third that of GFP-Nras and that GFP-Kras4B was rapidly associated with all membrane fractions, including those enriched for Golgi (not shown).

To examine the possibility that the interaction between the GFP tag and the various ras molecules might be responsible for the differential localization, we transfected cells with untagged N-, H-, and Kras4B and determined subcellular distribution by direct immunofluorescence (Figure 5C). We utilized CHO cells in these studies because their level of endogenous ras proved to be low relative to that observed in MDCK cells (Figure 1B), such that the ectopically expressed ras proteins could be specifically observed. The localization of the untagged ras molecules recapitulated that revealed by GFP-tagged ras molecules in live cells. Thus, the pattern of subcellular expression of Kras4B differed from that of Nras and Hras, suggesting that the two classes of ras gene products traffic differently.

To determine if the dual membrane targeting signals

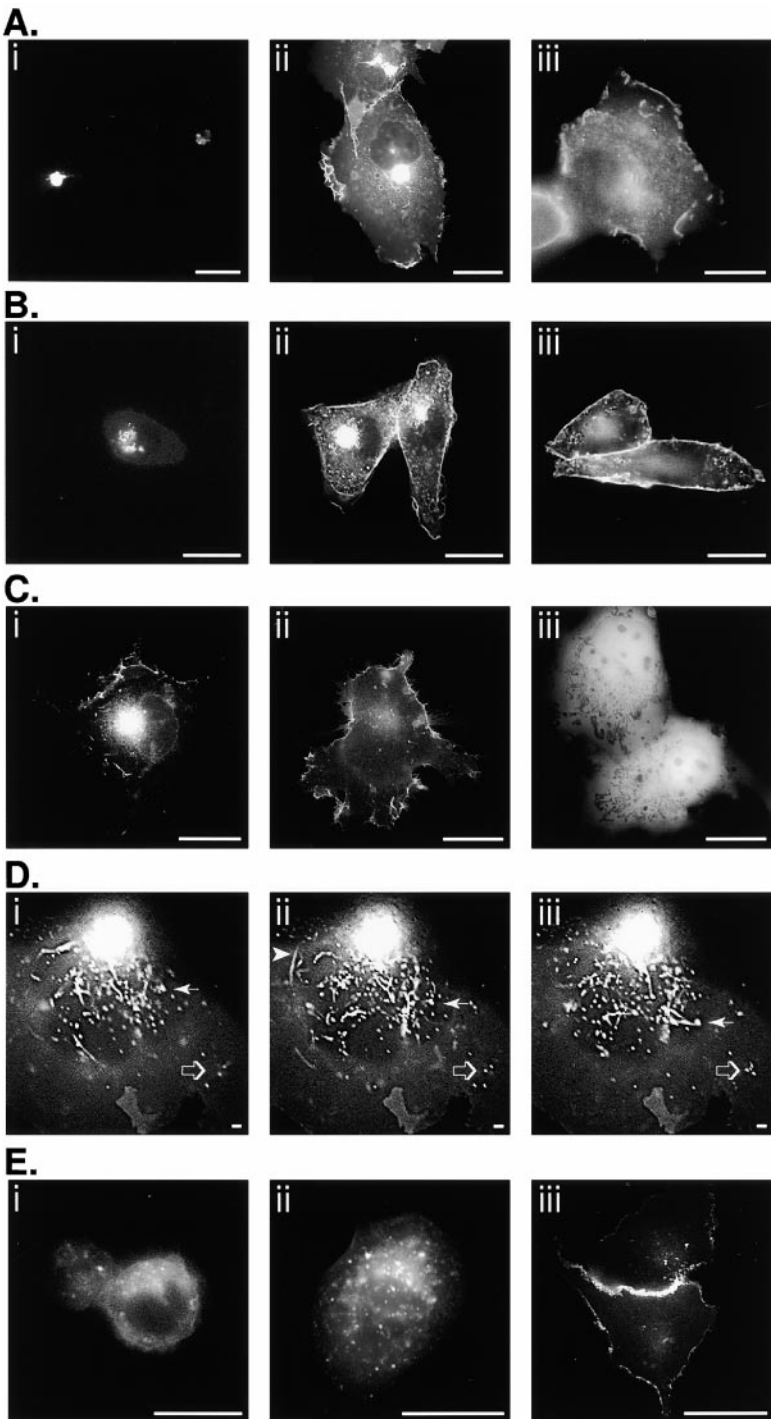

Figure 3. Trafficking of GFP-Nras

(A) COS-1 cells transiently transfected with GFP-Nras were examined alive at 8 hr (i) and 16 hr (ii) after transfection and after 5 hr of cycloheximide (50 μg/ml) treatment following 16 hr of expression (iii). Bars = 10 μm.

(B) A CHO cell line stably transfected with GFP-Nras under the control of an IPTG-inducible promotor was examined alive 8 hr (i) and 16 hr (ii) after the addition of IPTG and after 5 hr of cycloheximide treatment following 16 hr of IPTG induction (iii). Bars = 10 μm.

(C) COS-1 cells examined alive 24 hr after transient transfection with VSVG-GFP (i), Fyn-GFP (ii), and a ras CAAX mutant, GFP-NrasC186S (iii). Bars = 10 μm.

(D) High-magnification views of the peri-Golgi region of a GFP-Nras-transfected COS-1 cell imaged at successive 30 s intervals (i–iii), revealing motile fluorescent vesicles. The arrow indicates a vesicle moving away from the Golgi along a linear track. The open arrow indicates a cluster of vesicles that converge. The arrowhead indicates a tubulovesicular structure that appears transiently. Bars = 1 μm.

(E) CHO cell line in (B) treated with BFA for 8 hr beginning 3 hr after IPTG induction (i) and MDCK cells transiently transfected with GFP-Nras (ii) or Fyn-GFP (iii) treated with BFA for 8 hr beginning 3 hr after transfection. Bars = 10 μm.

described in the hypervariable domains of the various ras gene products are sufficient to account for the differential localization observed with GFP-tagged ras proteins, we tagged peptides corresponding to the three hypervariable regions with GFP (Figure 5D). GFP constructs extended at the C terminus with the last 11 amino acids (aa) of Nras, the last 10 aa of Hras, or the last 20 aa of Kras4B and gave patterns of fluorescence indistinguishable from those of the GFP-tagged full-length constructs. Thus, the hypervariable domains of ras gene products are necessary and sufficient to account for the differential localization of the full-length proteins. This suggests that each type of second signal (palmitoylation or a polybasic domain) directs ras proteins to alternative membrane targeting pathways.

The CAAX Motif Targets Proteins to the Endomembrane System

We confirmed that the CAAX motif is necessary for membrane targeting by demonstrating that GFP-NrasC186S (mutation in the CAAX cysteine) remained in the cytosol

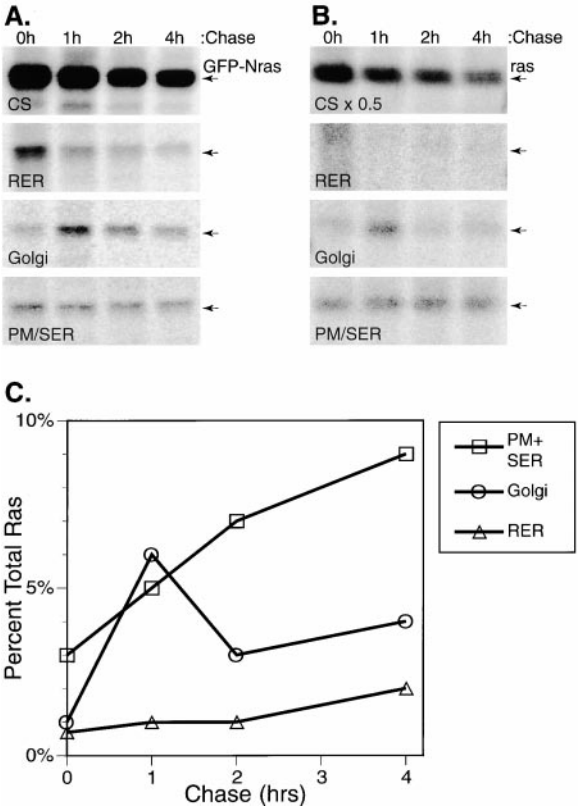

Figure 4. Subcellular Distribution after Chase of Pulse-Labeled Ras

(A) MDCK cells stably expressing GFP-Nras were pulse labeled (20 min) with [^{35}S]methionine, chased for the times indicated, homogenized, and separated into fractions enriched for cytosol (CS), rough microsomes (RER), Golgi, and PM + smooth microsomes (PM/SER). GFP-Nras was immunoprecipitated from detergent extracts of each fraction and analyzed by SDS-PAGE and phosphorimager. Results are representative of six experiments.

(B) Untransfected MDCK cells were analyzed for endogenous ras as in (A) using a pan-ras antibody. Results are representative of nine experiments.

(C) Immunoprecipitated ras shown in (B) was quantitated by phosphorimager and plotted as the percent of total ras recovered.

(Figure 3C$_{iii}$). To determine if the CAAX motif alone, previously shown to be insufficient for PM targeting (Hancock et al., 1991b), is sufficient for endomembrane targeting, we added the CAAX sequences of Nras, Hras, Kras, and the ras-related protein Rac1 to the C terminus of GFP. Each GFP-CAAX construct was not detected in the cytosol, but rather in the ER, nuclear envelope, and Golgi (Figure 6A). High-magnification, high-resolution images revealed a distinct localization on individual ER canaliculi extending to the periphery of the cell but completely excluding the PM (Figure 6A, right panels, and Figure 7A$_{ii}$). The localization of GFP-CLLL (Rac1 CAAX motif, Figure 6A$_{iii}$), a substrate for geranylgeranlytransferase type I rather than farnesyltransferase, was indistinguishable from that of the three ras CAAX motifs (GFP-CVVM, GFP-CVIM, and GFP-CVLS, Figures 6A$_{i}$, 6A$_{ii}$, and 7A$_{ii}$), demonstrating that endomembrane targeting by CAAX sequences is independent of the type of isoprenyl modification.

These data suggested that the second membrane targeting signal upstream of the CAAX motif is required not for endomembrane association but rather for subsequent ras trafficking out of the endomembrane system. To confirm this, we tagged with GFP an NrasC181S mutant in which the single palmitoylation site was removed, an HrasC181S,C184S double mutant in which both palmitoylation sites were removed, and a 20 aa Kras4B hypervariable domain in which the six contiguous lysines were changed to glutamines. Each construct was localized in the ER and Golgi but not in the PM (Figure 6B) in a pattern indistinguishable from that of the GFP-CAAX constructs (Figure 6A). Thus, palmitoylation or a polybasic domain do not simply act in conjunction with farnesylation to promote nonspecific membrane association, but rather are required for further trafficking of already membrane-associated ras molecules out of the endomembrane system.

Carboxyl Methylation Is Required for Ras Trafficking

The endomembrane targeting encoded by the CAAX motif together with the endomembrane localization of prenyl-CAAX processing enzymes suggests that further processing may regulate subsequent transport to the PM. To test this hypothesis, we studied the role of carboxyl methylation in membrane targeting of GFP-tagged ras proteins. To establish that our GFP-tagged ras proteins and CAAX constructs were substrates for pcCMT, we determined colocalization with pcCMT of prenylated GFP-CAAX proteins and analyzed the expressed fusion proteins for carboxyl methylation. We compared the subcellular localization of GFP-CAAX constructs to that of GFP-tagged pcCMT and found them to be remarkably similar (Figure 7A). To confirm the colocalization in the endomembrane system, we cotransfected COS-1 cells with the various GFP-CAAX constructs and pcCMT tagged with a FLAG epitope. Each GFP-CAAX construct colocalized with pcCMT-FLAG (Figure 7B).

We confirmed the fluorescence colocalization by demonstrating that the GFP-tagged ras proteins and CAAX-containing peptides served as substrates for pcCMT (Figure 7C). As expected, all GFP-tagged ras proteins were methylesterified on their α carboxyl group. Interestingly, whereas Nras and Hras were carboxyl methylated to a similar degree, the molar ratio of methyl group incorporation into GFP-Kras4B was almost twice that of the other ras gene products, indicating that, despite the predominantly PM steady-state pattern of GFP-Kras4B fluorescence (Figure 5), the recombinant protein must nonetheless have access to the endomembrane system, consistent with the endomembrane targeting of the Kras4B CAAX motif (Figure 6A$_{ii}$).

In contrast to the differential methylation of the full-length constructs, the CAAX motifs alone of each ras protein tagged with GFP were carboxyl methylated to a similar extent. Furthermore, the palmitoylation-deficient mutant of GFP-Nras was methylated to the same extent as the Nras CAAX motif alone. The extent of methylation of each of these constructs was roughly half that of the full-length ras proteins, suggesting that, whereas the second signal is not required for carboxyl methylation, it enhances the efficiency of this modification.

GFP-CLLL was methylated twice as efficiently as the farnesylated GFP-CAAX constructs, consistent with the higher rate constant of pcCMT for geranylgeranylated

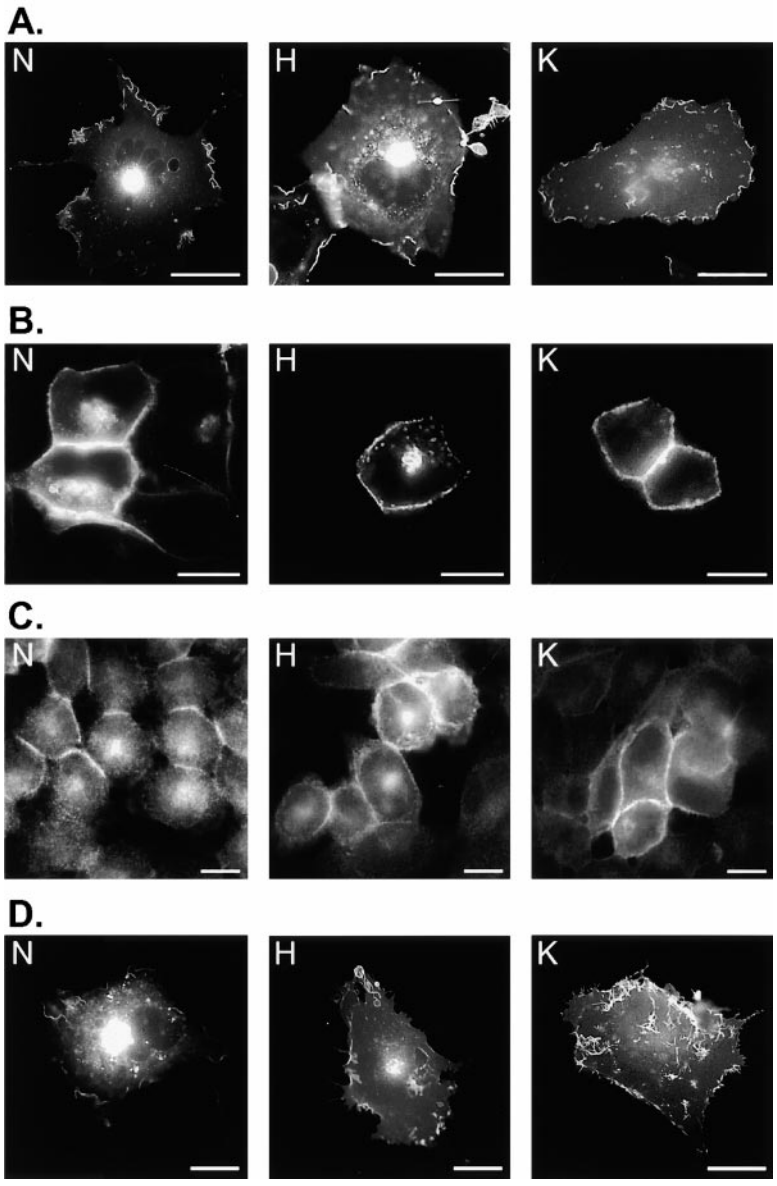

Figure 5. Differential Localization of GFP-Tagged Ras Proteins

(A) COS-1 cells and (B) MDCK cells transiently transfected with GFP-Nras (N), GFP-Hras (H), or GFP-Kras4B (K) and imaged alive.

(C) CHO cells transiently transfected with untagged Nras (N), Hras (H), or Kras4B (K), fixed, permeabilized, and stained with TRITC-conjugated Y13-258 antibody.

(D) COS-1 cells transiently transfected with GFP extended at the C terminus with the hypervariable domains (11, 10, and 20 aa, respectively) of Nras (N), Hras (H), or Kras4B (K) and imaged alive. Bars = 10 μm.

substrates (Pillinger et al., 1994) and suggesting that geranylgeranylated proteins may therefore have a higher affinity for the endomembrane system. As expected, prenylation was absolutely required for methylation, since the GFP-NrasC186S mutant was not methylated at all.

To determine if carboxyl methylation is required for membrane targeting of ras proteins, we treated COS-1 cells transfected with GFP-Nras or GFP-Kras4B with the pcCMT inhibitor *N*-acetyl-*S*-*trans*-farnesylcysteine (AFC) or a control prenylcysteine analog that does not inhibit pcCMT, *N*-acetyl-*S*-geranylcysteine (AGC), and observed the subcellular localization of the GFP-tagged ras molecules (Figure 7D). Whereas AGC did not affect the pattern of GFP-ras fluorescence, AFC altered the subcellular distribution of GFP-Nras and GFP-Kras4B in a dose-dependent fashion. Golgi and PM fluorescence were markedly diminished in cells treated with AFC. Moreover, the majority of cells treated with AFC revealed a cytosolic pattern of fluorescence never observed in untreated cells expressing GFP-ras but similar to that observed in cells expressing the unprocessed GFP-NrasC186S (Figure $3C_{iii}$) or GFP alone. Thus, carboxyl methylation and, by extension, the prerequisite AAX proteolysis are required for efficient trafficking of ras from the cytosol through the endomembrane system and on to the PM.

Discussion

Because ras has been reported to localize (Willingham et al., 1980) and function (Willumsen et al., 1984) at the PM, posttranslational processing of CAAX proteins has been understood as a process that mediates direct targeting of cytosolic proteins to the PM. The discovery that at least two of the enzymes that further modify prenylated CAAX proteins are restricted to the endomembrane system (Dai et al., 1998; Schmidt et al., 1998)

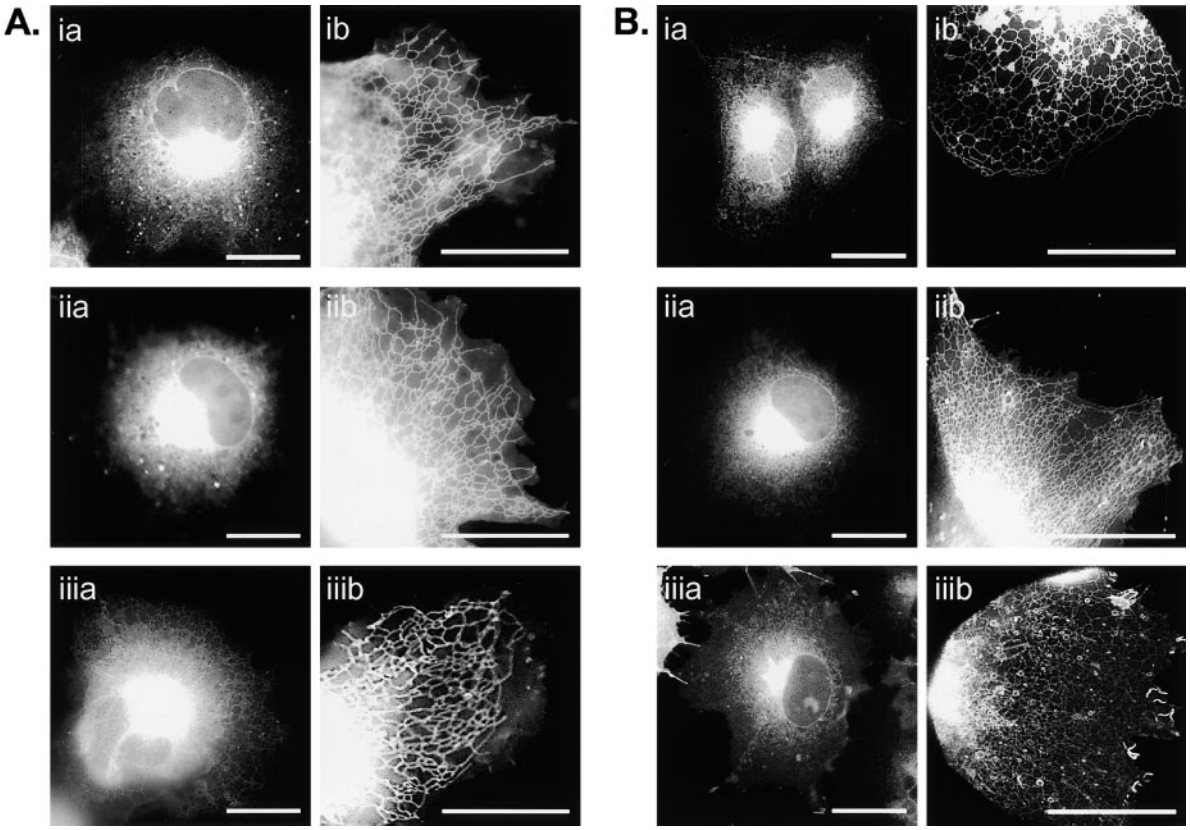

Figure 6. The CAAX Motif Targets Proteins to the Endomembrane System

(A) COS-1 cells transiently transfected with the CAAX motifs of Nras, Kras4B, or Rac1 tagged with GFP: GFP-CVVM (i), GFP-CVIM (ii), and GFP-CLLL (iii).

(B) COS-1 cells transiently transfected with GFP-tagged ras constructs in which the secondary membrane signal (palmitoylation or polybasic domain) was eliminated: GFP-NrasC181S (i), GFP-HrasC181S,C184S (ii), GFP-C-terminal 20 aa of Kras4B with the six contiguous lysines changed to glutamine (iii).

Left panels (a) show the entire cell; right panels (b) show high-magnification views of peripheral reticulum. Bars = 10 μm.

has provoked a revision in the assumptions about CAAX protein trafficking. Our data demonstrate that ras is indeed targeted to the endomembrane system. Moreover, the kinetics of Golgi versus PM expression of Nras reported by a fluorescent tag, the transient expression of pulse-labeled endogenous ras in Golgi fractions, the association of Nras and Hras with vesicles similar to those transporting VSVG protein, and the inhibition of PM expression of GFP-Nras following prolonged treatment with BFA suggest that PM association of these ras gene products is mediated by vesicular transport from the endomembrane system. Most compelling is our observation that the CAAX motif alone targets proteins specifically to the ER and Golgi and that the previously described second membrane targeting sequence is in fact required for further transport to the PM. This suggests that prenylated CAAX motifs generated in the cytosol through the action of prenyltransferases interact with specific receptors in the endomembrane system, where they are then accessible for further processing. Whether the putative vesicular transport from the endomembrane is mediated by components of the classical secretory pathway or a novel pathway remains to be determined. In either case, the topology is such that ras would be predicted to associate with the cytoplasmic face of the endomembrane and transport vesicles.

The original assignment of ras to the inner leaflet of the PM was made two decades ago on the basis of electron microscopic immunocytochemistry of cells transformed with the Harvey strain of murine sarcoma virus (Willingham et al., 1980). In retrospect, it is evident that the ultrastructural analysis in this study was limited to the apical surface of polarized MDCK cells where the assignment of ras to the inner leaflet of the PM was facilitated by interdigitating microvilli. It is unclear if Golgi cisternae were examined. Moreover, careful inspection of the immunofluorescent data presented in this study reveals, in addition to the PM staining that was reported, perinuclear expression of ras in both Mo-MuLV mouse cells and MDCK cells. Subsequently published immunofluorescent studies of ras are open to similar reinterpretation (Furth et al., 1982; Grand et al., 1987). In addition, mutations in the hypervariable domain of Hras have been reported that result in localization on internal membranes and diminished transforming activity (Willumsen et al., 1996). The vast majority of published studies that reported ras in the PM relied either on analysis of soluble (S100) versus insoluble (P100)

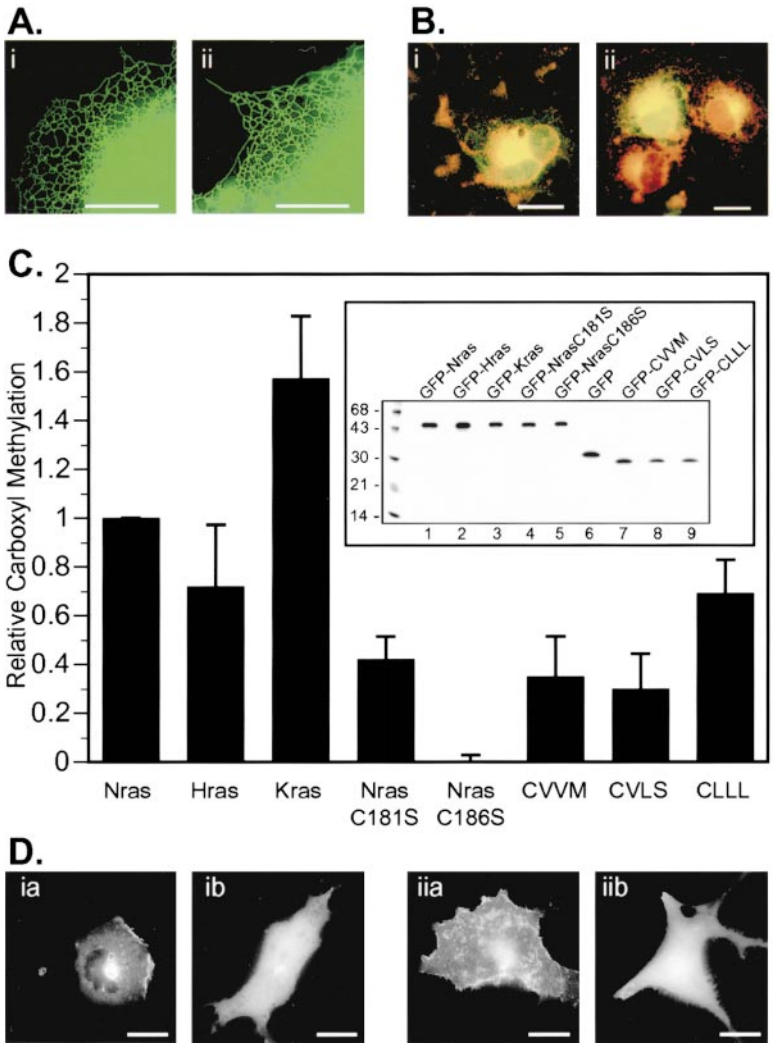

Figure 7. The Role of Carboxyl Methylation in Ras Trafficking

(A) COS-1 cells transiently transfected with pcCMT-GFP (i) or GFP-CVLS (CAAX motif of Hras) (ii).

(B) COS-1 cells cotransfected with GFP extended at the C terminus with the CAAX motifs of Nras (CVVM) (i) or Rac1 (CLLL) (ii) and pcCMT-FLAG were fixed and stained for the FLAG epitope (Texas red) and analyzed by dual color epifluorescence microscopy where yellow pseudocolor indicates colocalization.

(C) COS-1 cells transiently transfected with the indicated GFP constructs were metabolically labeled with [^{3}H-methyl]-L-methionine. GFP-tagged molecules were then immunoprecipitated from cell lysates (inset) and analyzed for carboxyl methylation by alkaline hydrolysis of gel slices. The values for carboxyl methylation (bar graph) were adjusted for amount of immunoprecipitated protein and normalized to GFP-Nras. n = 3.

(D) COS-1 cells transiently transfected with GFP-Nras (i) or GFP-Kras4B (ii) were treated beginning 2 hr posttransfection with 100 μM of a control prenylcysteine compound, AGC (a), or the methylation inhibitor AFC (b) and imaged alive after 24 hr. Bars = 10 μm.

subcellular fractions (Grand et al., 1987; Kato et al., 1992) or on Triton X-114 partition analysis (Hancock et al., 1989, 1990), neither of which can distinguish between proteins associated with the PM and those associated with other membrane compartments. Despite the numerous examples in the literature of immunolocalization of ras to the PM, an early study of pulse-labeled ras found that the predominant pool of nascent ras remained soluble up to 4 hr (Ulsh and Shih, 1984). Thus, both our observations that at steady-state ras is in the endomembrane system and that a large pool of nascent ras remains cytosolic are not inconsistent with the previous literature.

The seminal studies of Hancock and Marshall established that CAAX processing was necessary but not sufficient for PM localization of ras (Hancock et al., 1990, 1991b). Also required was a second signal in the hypervariable domain that consisted of either palmitoylation sites or a polybasic domain. The conclusions reached by these authors were based on solubility, Triton X-114 partition, and immunofluorescence. In retrospect, the localization revealed by indirect immunofluorescent analysis of palmitoylation-deficient and polybasic-neutralized mutants in fixed, permeabilized cells that was interpreted as cytosolic staining (Hancock et al., 1990) is in fact consistent with the endomembrane expression that we have documented in live cells when these same mutants were tagged with GFP. Thus, our data are consistent with those of Hancock, but we have further elucidated the requirements for membrane targeting of CAAX proteins by demonstrating that, whereas the CAAX motif alone is insufficient for PM localization, it is sufficient for endomembrane targeting. This observation has wide-ranging implications that include the suggestion of prenyl-CAAX membrane-binding sites in the ER, compartmentalized modification, vesicular transport of CAAX proteins, and signaling on intracellular membranes.

Our observation that the subcellular localization of Kras4B differs from that of Nras and Hras was unexpected. The Kras4B CAAX motif was indistinguishable from that of Nras and Hras in acting alone to direct GFP to the endomembrane. Moreover, GFP-Kras4B was carboxyl methylated to a higher stoichiometry than the other two ras gene products tagged with GFP, a modification that is restricted to the endomembrane system. Thus, it appears likely that Kras4B, like its homologs, transits the endomembrane compartment. One explanation for the apparent difference in the extent of Golgi expression among GFP-tagged ras proteins is that the kinetics and/or flux of endomembrane transit may be

distinct. Indeed, the cytosolic half-life of GFP-Kras was one-third that of GFP-Nras. The basis for a kinetic difference could be two distinct pathways of transport from the endomembrane system to the PM. For example, whereas palmitoylation of Nras and Hras might target these proteins to transport vesicles, the polybasic domain of Kras4B might specify an alternative pathway. Indeed, we observed vesicles similar to those illuminated by VSVG-GFP with GFP-Nras and GFP-Hras but not GFP-Kras4B. Supporting the notion of multiple membrane trafficking pathways for ras proteins is the recent observation that Kras4B, but not Nras or Hras, was associated with tubulin and that PM expression of GFP-Kras4B only was blocked by nocodazole, an agent that depolimerizes microtubules (Thissen et al., 1997).

Whereas carboxyl methylation significantly augments the affinity of farnesylated proteins for liposomes (Silvius and l'Heureux, 1994) and membranes (Hancock et al., 1991a), the increment is trivial in the case of geranylgeranylated proteins (Silvius and l'Heureux, 1994), suggesting that rather than simply adding to the C-terminal hydrophobicity of CAAX proteins, carboxyl methylation regulates specific protein–protein interactions in a reversible fashion. The requirement for carboxyl methylation of *S. cerevisiae* **a** factor for interaction with both its transporter (Ste6p) and receptor (Ste3p) supports this view (Marcus et al., 1991; Sapperstein et al., 1994). Our data demonstrate a biological role for prenylcysteine carboxyl methylation apart from the one it plays in the yeast mating pathway and demonstrate differential methylation of ras gene products (Kras4B $>$ Nras $=$ Hras). The predominantly cytosolic localization of both GFP-Nras and GFP-Kras4B in cells treated with a pcCMT inhibitor suggests that carboxyl methylation is required for efficient trafficking of ras through the endomembrane system, suggesting a mechanism for the reported inhibition of proliferation of ras- but not v-raf-transformed cells treated with pcCMT inhibitors (Marciano et al., 1995). Since pcCMT is restricted to the endomembrane system, one attractive model that fits the data is that pcCMT acts as one of the critical acceptor proteins for prenylated CAAX proteins, presumably those that have been acted upon by the ER-restricted AAX protease (Schmidt et al., 1998), and blockade of pcCMT with a competitive inhibitor therefore causes ras to accumulate in the cytosol. Carboxyl methylation could also regulate downstream events by mediating the interaction of ras proteins with elements of the transport pathways involved in further trafficking to the PM. The greater extent of methylation of wild type GFP-Nras relative to that of the GFP-NrasC181S palmitoylation-deficient mutant suggests that whereas palmitoylation is not required for carboxyl methylation, the two processes are linked.

Taken together, our data support a more complex model of ras membrane targeting than has been previously appreciated. In this model, farnesylated ras proteins interact with specific receptors in the endomembrane system, perhaps the prenylcysteine-CAAX protease itself, are acted upon by the endomembrane resident prenyl-CAAX processing enzymes, and are then released to one or more transport pathways that bring them to the PM. One corollary to this model is the possibility that palmitoylation specifies a pathway distinct from that followed by CAAX proteins containing a polybasic domain. Thus, rather than cumulatively conveying nonspecific hydrophobicity on otherwise hydrophilic proteins, the sequential events of CAAX processing regulate discrete stages of progress along a pathway. The compartmentalization and relative complexity of this model would allow for much greater regulation of the flux of ras to the PM. Recently developed inhibitors of farnesyltransferase show great potential as anti-cancer drugs (Gibbs and Oliff, 1997). The complexity of ras trafficking elucidated by our data suggests that membrane targeting of ras might be interrupted at multiple stages, raising the possibility of therapeutic synergy among inhibitors of the transport pathway developed to block oncogenic ras.

Experimental Procedures

Plasmid Constructs

The eukaryotic expression vectors pEGFP-C3 and pEGFP-N3 were obtained from Clontech, and pcDNA3.1 and pcDNA3.1/Hygro were from Invitrogen. The coding regions of N-, H- and Kras4B were generated by PCR from the respective cDNAs (gifts from J. Settleman and J. Hancock) and inserted into ApaI and BglII sites in the multiple cloning region of pEGFP-C3 (N-, H-, and Kras4B) and pcDNA3.1 (Hras). Alleles encoding C181S and C186S mutants of Nras and a C181S,C184S double mutant of Hras were constructed by site-directed mutagenesis and inserted likewise into pEGFP-C3. DNA encoding the C-terminal 20 aa of K-ras in which the six contiguous lysine codons were changed to encode six glutamines was generated by PCR from pEGFP-6QCCIL (kind gift of J. Hancock) and inserted into pEGFP-C3. DNA fragments of 33 bp or less used to produce the GFP-CAAX constructs were generated by synthesizing and gel purifying complementary $+$ and $-$ strand oligonucleotides that were annealed to form linear dsDNA and inserted into the ApaI and BglII sites of pEGFP-C3. pCMV3R-GFP-Nras encoding GFP-Nras under the control of a CMV promotor that incorporates multiple binding sites for the Lac repressor was constructed by replacing the coding region of luciferase with that of EGFP-Nras in pCMV3R-Luc (kind gift of M. Roth). pEGFP-381 and pEGFP-KiJ encoding the C-terminal 10 aa of Hras and 20 aa of Kras4B, respectively, fused to EGFP were kind gifts of J. Hancock. pCDM8-VSVG-GFP encoding the ts045 mutant of VSVG protein fused to EGFP was a kind gift of J. Lippincott-Schwartz. The coding region of Fyn (cDNA obtained from M. Resh) was inserted into the HindIII and BamHI sites of pEGFP-N3. A dsDNA encoding the 8 aa FLAG epitope was cloned into the XbaI and ApaI sites of pcDNA3.1/Hygro to generate pcDNA3.1/Hygro-FLAG, and the coding region of pcCMT was then subcloned in-frame into the EcoRI and XbaI sites of the resulting plasmid.

Antibodies and Reagents

Rabbit polyclonal anti-GFP antibody was obtained from Clontech, mouse monoclonal anti-Flag antibody was obtained from Sigma, rabbit polyclonal anti-rat liver mannosidase II was obtained from K. Moreman, rat monoclonal anti-Hras antibodies Y13-258 and Y13-259 were obtained from Santa Cruz Biotechnology, and anti-CD 20 control monoclonal antibody was from D. Scheinberg. Texas red–conjugated donkey anti-rabbit and anti-mouse secondary antibodies were obtained from Jackson Labs. Anti-ras monoclonal Y13-238 and an irrelevant control monoclonal antibody (anti-CD20) were directly conjugated with TRITC (Pierce) according to the manufacturer's instructions. BFA, cycloheximide, and IPTG were obtained from Sigma. *N*-acetyl-*S*-farnesyl-L-cysteine (AFC) and *N*-acetyl-*S*-geranyl-L-cysteine (AGC) were obtained from Biomol. BODIPY TR-ceramide was obtained from Molecular Probes. Lipofectamine was purchased from Life Technologies.

Tissue Culture and Cell Lines

COS-1, CHO, and MDCK cells were maintained in 5% CO_2 at 37°C in Dulbecco's modified minimal essential medium containing 10%

fetal bovine serum. Stably transfected lines of CHO cells that express GFP-Nras under the control of an IPTG-inducible promotor were generated by G418 and flow cytofluorometric selection after transfection with pCMV3R-EGFP-Nras of a CHO cell line that constitutively expresses Lac repressor (gift of M. Roth). Stably transfected lines of MDCK cells that express GFP-Nras or GFP-Kras were selected by G418 and flow cytofluorometric selection.

Immunofluorescence and Fluorescence Microscopy

Cells for immunofluorescence were plated into 6-well trays (6 × 35 mm) at a density of 2×10^5 cells per well, containing four coverslips per well. The cells were transfected the next day using lipofectamine. Cells on coverslips were fixed with 4% paraformaldehyde, permeabilized with 0.2% Triton X-100, blocked with 5% milk/0.5% Tween in PBS, stained with TRITC-conjugated Y13-238 or anti-CD20 or with anti-Flag or anti-mannosidase II antibodies followed by Texas red–conjugated secondary antisera, and mounted on glass slides with Mowiol. Live cells for epifluorescence microscopy were plated likewise into 35 mm dishes containing a glass coverslip–covered 15 mm cutout (MatTek) and transfected the next day. Cells were examined 5–48 hr posttransfection with a Zeiss Axioscope epifluorescence microscope equipped with a Princeton Instruments cooled CCD camera and MetaMorph digital imaging software (Universal Imaging). Colocalization of mannosidase II with GFP-Nras was analyzed with a Molecular Dynamics confocal microscope.

Immunoelectron Microscopy

Thin frozen sections of COS-1 cells transfected with GFP-Nras were obtained (Croze et al., 1989) and processed for immunogold labeling as described (Liou et al., 1996) using anti-GFP antiserum and protein A–gold 10 nm conjugates. Observations were made on JEOL electron microscope JEM-1200 EX II at 80 kV.

Subcellular Fractionation

MDCK cells were grown to 90% confluence, incubated in methionine/cysteine–free DMEM with 10% dialyzed FBS for 30 min, labeled with 100 μCi/ml Easy Tag Express-[^{35}S] (NEN) for 20 min, chased with methionine/cysteine–replete medium for various times, and washed in ice-cold PBS prior to harvesting. Unlabeled cells were processed in parallel to generate fractions for marker enzyme analysis. Labeled (10^7) and unlabeled (10^6) cells were then suspended in homogenizing buffer (10 mM HEPES [pH 7.5], 10 mM KCl, 1 mM DTT, protease inhibitors), disrupted in a tight-fitting Dounce homogenizer with 30 strokes, and then adjusted to 0.25 M sucrose. To remove unbroken cells and nuclei, the homogenate was centrifuged at 600 × g for 5 min, and the resulting pellet was resuspended in homogenizing buffer, rehomogenized, and again centrifuged at 600 × g for 5 min. Mitochondria were removed from the combined 600 × g supernatants by centrifugation at 8000 × g for 10 min. Membrane and soluble fractions of the 8000 × g supernatant were separated by centrifugation at 160,000 × g for 90 min. The membrane pellet was resuspended in 1.25 M sucrose and separated by floatation through a discontinuous sucrose density gradient (0.25, 1.00, and 1.25 M) by centrifugation (350,000 × g for 120 min). Unlabeled fractions were analyzed for protein (Bio-Rad DC assay), RNA (Fleck and Munro, 1962), Na/K ATPase (Esmann, 1988), and galactosyl transferase (Fleisher et al., 1969) and pcCMT (Philips and Pillinger, 1995) activities as described. Labeled fractions were extracted with RIPA buffer, an aliquot was precipitated with hot 20% TCA for total counts, and ras was immunoprecipitated from the remainder with Y13-259-conjugated Sepharose beads (Santa Cruz Biotechnology) or anti-GFP antiserum (Clontech) followed by protein A–conjugated agarose. Immunoprecipitated ras was quantitated by phosphorimager.

Methylation Assay

COS-1 cells were seeded in 6-well trays at a density of 10^5 cells per well and transfected with EGFP or EGFP-CAAX fusion constructs using lipofectamine according to the manufacturer's instructions. Cells were methionine starved for 30 min at 24 hr posttransfection and labeled with 100 μCi/ml [^{3}H-methyl]-L-methionine for 30 min. Cells were then washed twice in PBS, lysed in 1 ml RIPA buffer (20 mM Tris [pH 7.5], 0.15 M NaCl, 1% NP-40, 0.1% SDS, 0.1% Na-DOC, 0.5 mM EDTA, 10 μg/ml leupeptin, 1 mM PMSF, 27 μg/ml aprotinin, 1 mM DTT), and immunoprecipitated with anti-GFP antiserum followed by protein A–conjugated agarose beads (Life Technologies). Beads were washed and eluted in sample buffer. Eluates were analyzed by 14% Tris-glycine SDS-PAGE (Novex) and immunoprecipitated proteins identified by fluorography. Bands corresponding to EGFP-CAAX fusion proteins were excised, and carboxyl methylation was quantitated by alkaline hydrolysis (1 N NaOH) and measurement of vapor phase [^{3}H]methanol as described (Philips and Pillinger, 1995).

Acknowledgments

We thank John Hancock, Jeffrey Settleman, Jennifer Lippincot-Schwartz, and Marilyn Resh for generously providing plasmids. We are grateful to Michael Roth for supplying the IPTG inducible expression system and to Kelly Moreman and David Scheinberg for antibodies. We thank Gordon Fishell for expert instruction on digital epifluorescence microscopy and John Weider and Joe Frey for digital graphics support. We thank Pheobe Recht for help with tissue culture and Iwona Gumper for the immunoelectron microscopy. We thank David Sabatini for his critical reading of the manuscript. This work was supported by grants from the National Institutes of Health (AI36224, GM55279, NCRR M01 RR00096, and T32 GM07308).

Received February 12, 1999; revised June 4, 1999.

References

Boyartchuk, V.L., Ashby, M.N., and Rine, J. (1997). Modulation of Ras and **a**-factor function by carboxyl-terminal proteolysis. Science *275*, 1796–1800.

Casey, P.J., and Seabra, M.C. (1996). Protein prenyltransferases. J. Biol. Chem. *271*, 5289–5292.

Clarke, S. (1992). Protein isoprenylation and methylation at carboxyl terminal cysteine residues. Annu. Rev. Biochem. *61*, 355–386.

Croze, E., Ivanov, I.E., Kreibich, G., Adesnik, M., Sabatini, D.D., and Rosenfeld, M.G. (1989). Endolyn-78, a membrane glycoprotein present in morphologically diverse components of the endosomal and lysosomal compartments: implications for lysosome biogenesis. J. Cell Biol. *108*, 1597–1613.

Dai, Q., Choy, E., Chiu, V., Romano, J., Slivka, S., Steitz, S., Michaelis, S., and Philips, M.R. (1998). Mammalian prenylcysteine carboxyl methyltransferase is in the endoplasmic reticulum. J. Biol. Chem. *273*, 15030–15034.

Esmann, M. (1988). ATPase and phosphatase activity of Na+,K+-ATPase: molar and specific activity, protein determination. Methods Enzymol. *156*, 105–115.

Fleck, A., and Munro, H.N. (1962). The precision of ultraviolet absorption measurement in the Schmidt-Thannhauser procedure for nucleic acid determination. Biochim. Biophys. Acta *55*, 571–583.

Fleisher, B., Fleisher, S., and Osawa, H. (1969). Isolation and characterization of Golgi membranes from bovine liver. J. Cell Biol. *43*, 59–79.

Fujimura-Kamada, K., Nouvet, F.J., and Michaelis, S. (1997). A novel membrane-associated metaloprotease, Ste24p, is required for the first step of NH_2-terminal processing of the yeast **a**-factor precursor. J. Cell Biol. *136*, 271–285.

Furth, M.E., Davis, L.J., Fleurdelys, B., and Scolnick, E.M. (1982). Monoclonal antibodies to p21 products of the transforming gene of Harvey murine sarcoma virus and of the cellular ras gene family. J. Virol. *43*, 294–304.

Gibbs, J.B., and Oliff, A. (1997). The potential of farnesyltransferase inhibitors as cancer chemotherapeutics. Annu. Rev. Pharmacol. Toxicol. *37*, 143–166.

Grand, R.J., Smith, K.J., and Gallimore, P.H. (1987). Purification and characterisation of the protein encoded by the activated human N-ras gene and its membrane localisation. Oncogene *1*, 305–314.

Hancock, J.F., Magee, A.I., Childs, J.E., and Marshall, C.J. (1989).

All ras proteins are polyisoprenylated but only some are palmitoylated. Cell *57*, 1167–1177.

Hancock, J.F., Paterson, H., and Marshall, C.J. (1990). A polybasic domain or palmitoylation is required in addition to the CAAX motif to localize p21^{ras} to the plasma membrane. Cell *63*, 133–139.

Hancock, J.F., Cadwallader, K., and Marshall, C.J. (1991a). Methylation and proteolysis are essential for efficient membrane binding of prenylated p21$^{K\text{-}ras(B)}$. EMBO J. *10*, 641–646.

Hancock, J.F., Cadwallader, K., Paterson, H., and Marshall, C.J. (1991b). A CAAX or a CAAL motif and a second signal are sufficient for plasma membrane targeting of ras proteins. EMBO J. *10*, 4033–4039.

Kasinathan, C., Grzelinska, E., Okazaki, K., Slomiany, B.L., and Slomiany, A. (1990). Purification of protein fatty acyltransferase and determination of its distribution and topology. J. Biol. Chem. *265*, 5139–5144.

Kato, K., Cox, A.D., Hisaka, M.M., Graham, S.M., Buss, J.E., and Der, C.J. (1992). Isoprenoid addition to Ras protein is the critical modification for its membrane association and transforming activity. Proc. Natl. Acad. Sci. USA *89*, 6403–6407.

Liou, W., Geuze, H.J., and Slot, J.W. (1996). Improving structural integrity of cryosections for immunogold labeling. Histochem. Cell Biol. *106*, 41–58.

Lippincott-Schwartz, J., Yuan, L.C., Bonifacino, J.S., and Klausner, R.D. (1989). Rapid redistribution of Golgi proteins into the ER in cells treated with brefeldin A: evidence for membrane cycling from Golgi to ER. Cell *56*, 801–813.

Marciano, D., Ben-Baruch, G., Marom, M., Egozi, Y., Haklai, R., and Kloog, Y. (1995). Farnesyl derivatives of rigid carboxylic acids-inhibitors of ras-dependent cell growth. J. Med. Chem. *38*, 1267–1272.

Marcus, S., Caldwell, G.A., Miller, D., Xue, C.B., Naider, F., and Becker, J.M. (1991). Significance of C-terminal cysteine modifications to the biological activity of the *Saccharomyces cerevisiae* **a**-factor mating pheromone. Mol. Cell. Biol. *11*, 3603–3612.

Philips, M.R., and Pillinger, M.H. (1995). Prenylcysteine-directed carboxyl methyltransferase activity in human neutrophil membranes. Methods Enzymol. *256*, 49–63.

Pillinger, M.H., Volker, C., Stock, J.B., Weissmann, G., and Philips, M.R. (1994). Characterization of a plasma membrane-associated prenylcysteine-directed α carboxyl methyltransferase in human neutrophils. J. Biol. Chem. *269*, 1486–1492.

Presley, J.F., Cole, N.B., Schroer, T.A., Hirschberg, K., Zaal, K.J.M., and Lippincott-Schwartz, J. (1997). ER-to-Golgi transport visualized in living cells. Nature *389*, 81–85.

Reiss, Y., Goldstein, J.L., Seabra, M.C., Casey, P.J., and Brown, M.S. (1990). Inhibition of purified p21*ras* farnesyl:protein transferase by Cys-AAX tetrapeptides. Cell *62*, 81–88.

Romano, J.D., Schmidt, W.K., and Michaelis, S. (1998). The Saccharomyces cerevisiae prenylcysteine carboxyl methyltransferase Ste14p is in the endoplasmic reticulum membrane. Mol. Biol. Cell *9*, 2231–2247.

Sapperstein, S., Berkower, C., and Michaelis, S. (1994). Nucleotide sequence of the yeast STE14 gene, which encodes farnesylcysteine carboxyl methyltransferase, and demonstration of its essential role in **a**-factor export. Mol. Cell. Biol. *14*, 1438–1449.

Schmidt, W.K., Tam, A., Fujimura-Kamada, K., and Michaelis, S. (1998). Endoplasmic reticulum membrane localization of Rce1p and Ste24p, yeast proteases involved in carboxyl-terminal CAAX protein processing and amino-terminal α-factor cleavage. Proc. Natl. Acad. Sci. USA *95*, 11175–11180.

Silvius, J.R., and l'Heureux, F. (1994). Fluorimetric evaluation of the affinities of isoprenylated peptides for lipid bilayers. Biochemistry *33*, 3014–3022.

Thissen, J.A., Gross, J.M., Subramanian, K., Meyer, T., and Casey, P.J. (1997). Prenylation-dependent association of Ki-Ras with microtubules. Evidence for a role in subcellular trafficking. J. Biol. Chem. *272*, 30362–30370.

Ulsh, L.S., and Shih, T.Y. (1984). Metabolic turnover of human c-rasH p21 protein of EJ bladder carcinoma and its normal cellular and viral homologs. Mol. Cell. Biol. *4*, 1647–1652.

van't Hof, W., and Resh, M.D. (1997). Rapid plasma membrane anchoring of newly synthesized p59^{fyn}: selective requirement for NH2-terminal myristoylation and palmitoylation at cysteine-3. J. Cell Biol. *136*, 1023–1035.

Willingham, M.C., Pastan, I., Shih, T.Y., and Scolnick, E.M. (1980). Localization of the src gene product of the Harvey strain of MSV to plasma membrane of transformed cells by electron microscopic immunocytochemistry. Cell *19*, 1005–1014.

Willumsen, B.M., Norris, K., Papageorge, A.G., Hubbert, N.L., and Lowy, D.R. (1984). Harvey murine sarcoma virus p21 ras protein: biological and biochemical significance of the cysteine nearest the carboxy terminus. EMBO J. *3*, 2581–2585.

Willumsen, B.M., Cox, A.D., Solski, P.A., Der, C.J., and Buss, J.E. (1996). Novel determinants of H-Ras plasma membrane localization and transformation. Oncogene *13*, 1901–1909.